JOURNAL OF MATERIALS SCIENCE 27 (1992) 817–824

Mechanical properties of amorphous alloy compacts prepared by different consolidation techniques

M. TAKAGI
Research and Development Department, Nippondenso Co. Ltd, Showa-cho, Kariya, Aichi, 448 Japan

Y. KAWAMURA
Institute for Materials Research, Tohoku University, Katahira 2-2-1, Aoba-ku, Sendai, 980 Japan

T. IMURA
Department of Mechanical Engineering, Aichi Institute of Technology, Yachigusa, Yagusa-cho, Toyota, 470-03 Japan

J. NISHIGAKI, H. SAKA
Department of Materials Science and Engineering, Faculty of Engineering, Nagoya University, Furo-cho, Chikusa-ku, Nagoya, 464-01 Japan

Amorphous alloy compacts of $Fe_{78}B_{13}Si_9$ prepared by three different techniques (explosive consolidation, high hydrostatic pressure consolidation and warm extrusion) were deformed in compression between 573 and 723 K at a strain rate ranging from 8.3×10^{-5}–$4.2 \times 10^{-4} s^{-1}$. Explosively consolidated compacts had high strength ranging from 1.9–2.5 GPa below 623 K and could be plastically deformed to a strain of more than 50% at 673 K while preserving the amorphous state. Amorphous alloy compacts prepared by high hydrostatic pressure consolidation showed lower compressive strength. Those produced by warm extrusion were anisotropic in strength, the highest strength being as high as 2.74 GPa. It was also found that the geometry of the starting powders had a profound effect on the strength of the product compacts. Compacts prepared from flaky powders were stronger than those prepared from spherical ones. It is concluded that the mechanical properties of the amorphous alloy compacts depend on the consolidation technique, powder geometry and surface conditions of the powders, especially existence of oxide films.

1. Introduction

Amorphous alloys have various useful properties such as high strength, soft magnetism, and high corrosion resistance. The shapes of these alloys, however, are limited mainly to ribbons, wires, powders, or thin film, because of a high quenching rate generally required to preserve the amorphous state from liquid state. This imposes serious limitations on the fields of application of amorphous alloys.

In order to make full use of the potentially useful properties of amorphous alloys and extend the industrial applications, it is vital to prepare amorphous alloys in a bulky form. Many research works have been carried out to prepare amorphous alloy compacts [1–15]. One of the most promising techniques is consolidation of amorphous alloy powders. Amorphous alloy compacts whose density is as high as 99.7% or more of the corresponding amorphous alloy ribbons, have been successfully prepared by the present authors using the following techniques: (1) explosive consolidation, (2) high hydrostatic pressure consolidation, and (3) warm extrusion. Preliminary results on the consolidation techniques and the magnetic properties of the amorphous alloy compacts thus prepared have been reported [13–15].

Mechanical properties of the amorphous alloy compacts are also important factors in applying these materials as high-strength and wear-resistant materials. However, few systematic studies have been carried out on the effect of preparation techniques on the mechanical properties of amorphous alloy compacts for industrial use.

In the present study, the mechanical properties of amorphous alloy compacts of $Fe_{78}B_{13}Si_9$ prepared by the three different consolidation techniques were investigated systematically using compression tests. The results were compared with those obtained, using tensile tests, on the as-splat-quenched amorphous

0022–2461/92 $03.00 + .12

alloy ribbons of similar composition. Effects of consolidation technique and powder geometry on the bonding between the powders were studied.

2. Experimental procedure

The material investigated in this study was an $Fe_{78}B_{13}Si_9$ amorphous alloy, which has been used as a magnetic material and also has high strength. Two kinds of amorphous alloy powder were used as starting powders. One was a flaky powder, approximately 20 μm thick, 30–100 μm wide, and 50–200 μm long; these were obtained by grinding amorphous alloy ribbons produced by splat quenching. The other was a spherical powder 10–100 μm diameter; these were prepared by a rotating water-atomization method [16].

Three different consolidation techniques, i.e. explosive consolidation, high hydrostatic pressure consolidation, and warm extrusion, were used to compact the amorphous alloy powders. Details of these consolidation techniques have been published previously [13–15] and only a brief summary is given here. Explosively consolidated amorphous alloy compacts with a density close to that of the ribbon were made under a detonation pressure of approximately 10 GPa and a detonation velocity of 3000 m s^{-1}. High hydrostatic pressure consolidation was conducted using a cubic-type anvil apparatus. The amorphous alloy compacts with 100% density of the parent ribbon were obtained under a pressure of 5.4 GPa maintained at 723 K for 2 h. Here, use was made of the phenomenon where the crystallization temperature was higher under high pressure [14]. The amorphous alloy compacts with a density as high as 99.9% of that of the ribbons, were prepared by warm extrusion at 673 K of a billet of powders packed in a cylindrical container with a core of suitable material and diameter. Table I summarizes the four kinds of amorphous alloy compact used in this study.

Mechanical properties of the amorphous alloy compacts were measured by compression test. The rectangular specimens, 1 mm × 1 mm × 2 mm, were sectioned from the compacts using a spark machine. The surfaces of the specimens were polished mechanically with diamond powders. The specimens were compressed in vacuum between two tungsten carbide platens on an Instron-type testing machine at a strain rate between 8.3×10^{-5} and 4.2×10^{-4} s^{-1} and at a temperature from room temperature to 773 K. The specimens were annealed at the test temperature for 30 min prior to the compression test.

After compression tests, the specimens were examined by X-ray diffraction. The shape of the specimens after deformation or failure and the morphology of the internal powder particles were investigated by optical microscopy. The fracture surfaces were observed using a scanning electron microscope (SEM). Chemical composition of interfaces between powders in the as-consolidated materials was studied with an electron probe micro-analyser (EPMA).

TABLE I The amorphous alloy compacts used in this study

Specimen	Consolidation technique	Powder geometry
EF	Explosive consolidation	Flaky
ES	Explosive consolidation	Spherical
HF	High hydrostatic pressure consolidation	Flaky
WF	Warm extrusion	Flaky

3. Results

3.1. Explosively consolidated amorphous alloy compacts

3.1.1. Flaky powder compacts

Amorphous alloy compacts prepared by explosive consolidation using flaky powders (EF) were deformed in compression. Fig. 1 shows the stress–strain curves measured at different temperatures at a strain rate of $8.3 \times 10^{-5} s^{-1}$. At room temperature and 573 K, the specimens had comparably high strength of 1.9–2.0 GPa and failed without large deformation. A high strength of 2.45 GPa was obtained at 623 K. Above 673 K, strength of the compacts decreased with increasing temperature, and the compacts could be deformed to a strain of more than 50% before fracture.

Fig. 2 shows the temperature dependence of the maximum strain obtained in compression. It is clear that the amorphous alloy compacts of $Fe_{78}B_{13}Si_9$ soften abruptly above 623 K.

Fig. 3 shows X-ray diffraction (XRD) patterns taken on the specimens after deformation at (a) 673 K, (b) 723 K, and (c) 773 K. For compression tests below 673 K, the specimens remained amorphous, while above 723 K crystallization occurred during the test.

Overall views of the cross-section and morphology of internal powders of the specimens after being deformed in compression are shown in Fig. 4. When the specimens were compressed at 623 K, fracture occurred at an angle of approximately 40° to the compression axis, and the morphology of the powders remained unchanged during fracture. Above 673 K, however, the compacts deformed considerably except for the circumference, and the flaky particles became thin and elongated in a direction perpendicular to the

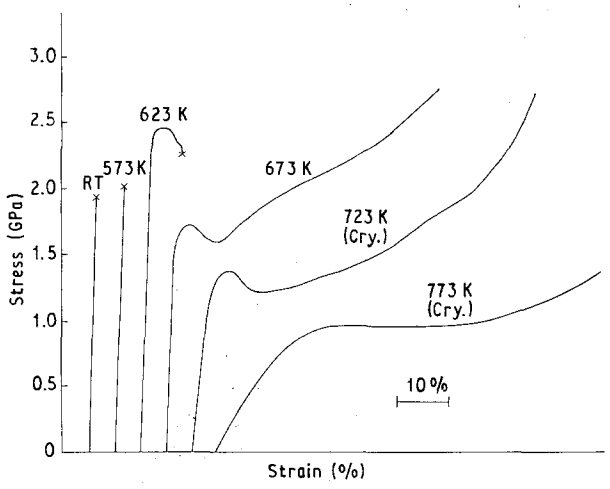

Figure 1 Compressive stress–strain curves of explosively consolidated compacts tested at different temperatures.

compression axis. In other words, the powders themselves deformed plastically, leading to a large overall plastic deformation of the compacts.

Fig. 5 shows scanning electron micrographs of the fracture surfaces of the amorphous alloy compacts. Interparticle fracture occurred predominantly at room temperature. In contrast, at 623 K transparticle fracture occurred, and much elongated vein patterns were observed; this was formed presumably by shear stress acting on the softened amorphous alloy.

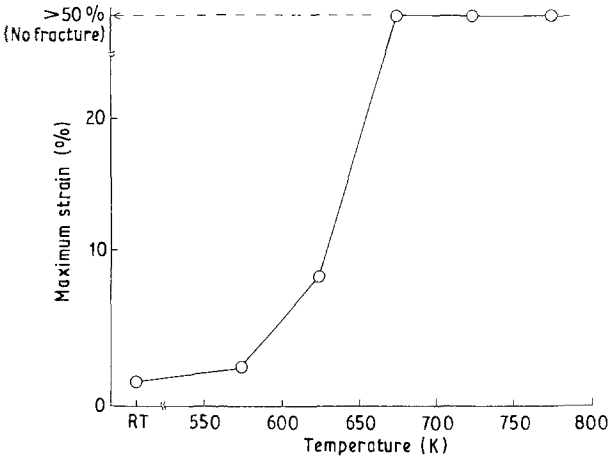

Figure 2 Temperature dependence of maximum strain obtained in compression test of the compacts EF, at $\dot{\varepsilon} = 8.33 \times 10^{-5} s^{-1}$.

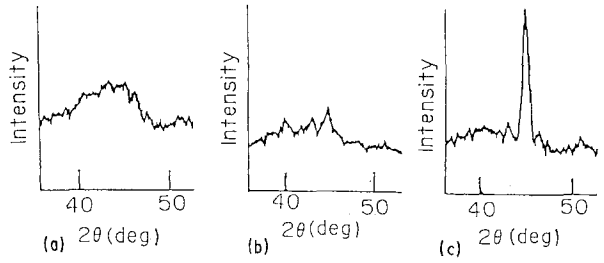

Figure 3 XRD patterns of explosively consolidated amorphous alloy compacts after compression test.

Fig. 6 shows the effect of temperature and strain rate on the deformation characteristics of the amorphous alloy compacts. Large plastic deformation to a strain of more than 50% while preserving the amorphous state was possible at 673 K at a strain rate between 8.3×10^{-5} and $2.5 \times 10^{-4} s^{-1}$. The yield stress, σ_y, or fracture stress, σ_f, of the amorphous alloy compacts did not change very much with increasing strain rate at 673 K, while those of the crystallized compacts increased slightly with increasing strain rate at 723 K.

3.1.2. Effect of shape of starting powders on the strength of the compacts

The temperature dependence of compressive strength of explosively consolidated amorphous alloy compacts prepared from flaky powder (EF) and from spherical powder (ES) is shown in Fig. 7. The strength of the spherical powder compacts ES was apparently lower than that of the flaky powder compacts EF.

Fig. 8 shows a scanning electron micrograph of the facture surface of the spherical powder compact ES tested at 623 K. Interparticle fracture was dominant in this case; this contrasts sharply with the case of the compact EF where transparticle fracture was dominant as shown in Fig. 5b. The shape of the starting powder affects the bonding between powders during the consolidation; powders with a flaky shape produce a better bonding than those with a spherical shape.

3.2. Amorphous alloy compacts prepared by high hydrostatic pressure consolidation

Amorphous alloy compacts prepared by high hydrostatic pressure consolidation (HF) were also deformed in compression. These results are also shown in Fig. 7. Only flaky powders were used, except for explosive

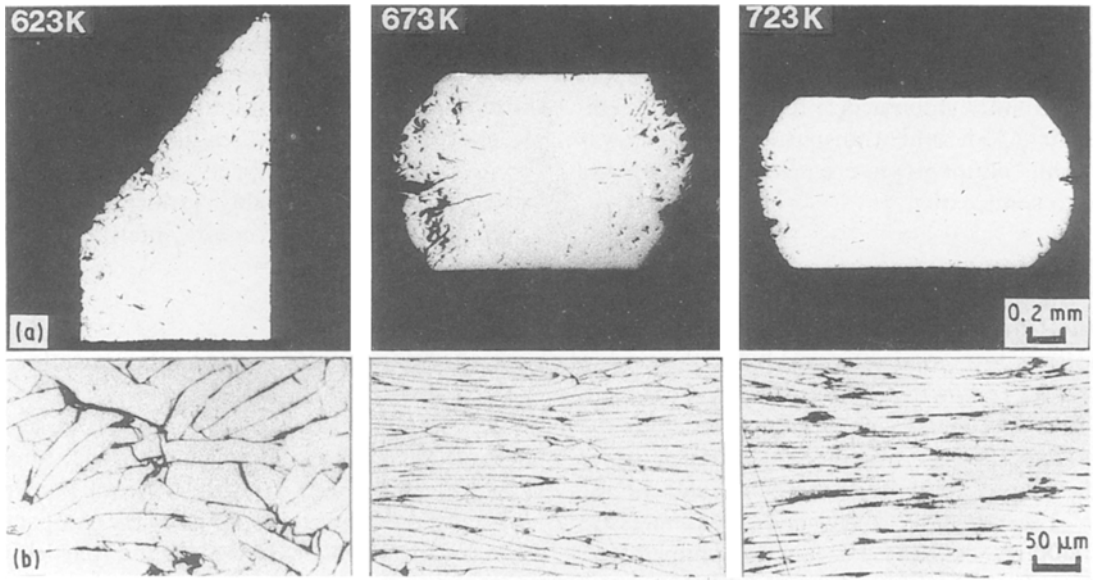

Figure 4 Optical micrographs showing (a) the outer shapes of the compacts and (b) the morphology of the internal powders (etched) after deformation at different temperatures.

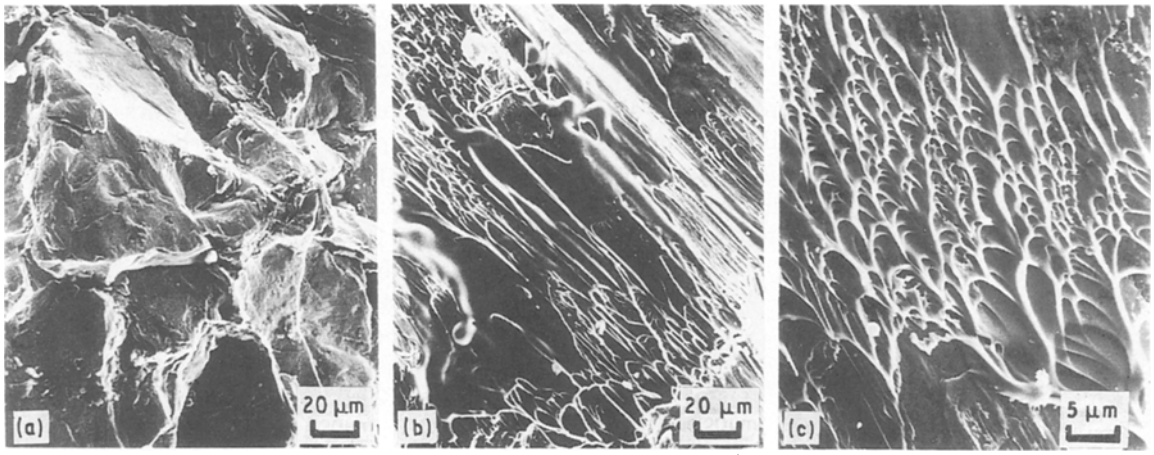

Figure 5 SEM images of fracture surfaces of explosively consolidated amorphous alloy compacts failured at (a) room temperature and (b, c) 623 K.

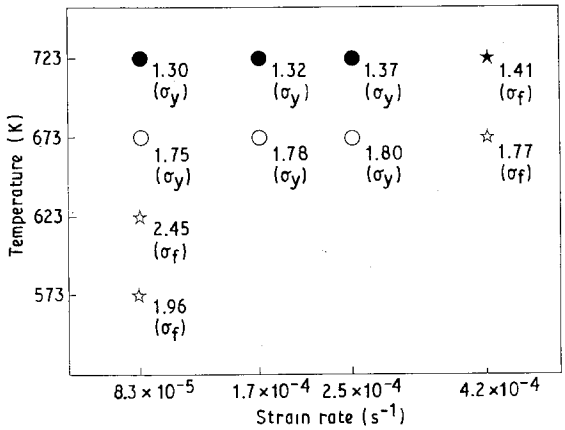

Figure 6 The effect of temperature and strain rate on the deformation characteristics of explosively consolidated amorphous alloy compacts. The subscripts denote yield stress, σ_y, and fracture stress, σ_f (GPa). (○) 50% deformed, amorphous; (●) 50% deformed, crystalline; (☆) fractured, amorphous; (★) fractured, crystalline.

consolidation, for the reason described in the preceding section. The temperature dependence of the strength of the compacts HF was similar to that of the explosively consolidated compact EF but at lower strength level. Fracture surfaces of the compacts HF were observed using SEM (see Fig. 9). The compact HF fractured in the interparticle region at room temperature. At 623 K, the transparticle fracture was predominant, although interparticle fracture was observed to some extent.

3.3. Amorphous alloy compacts prepared by warm extrusion

Amorphous alloy compacts produced by warm extrusion (WF) showed an anisotropy in strength (Fig. 7). The specimens compressed parallel to the extrusion axis, WF(||), fractured at a much lower stress than those compressed perpendicular to the extrusion axis, WF(⊥), which had a compressive strength as large as 2.74 GPa at room temperature. The fracture surfaces of the compacts WF(||) were parallel to the compression axis. It is evident that WF(||) fractured by the tensile stress which acted perpendicular to the compression axis. On the other hand, compacts WF(⊥) fractured in an irregular way.

The morphology of the fracture surface of the compacts WF(⊥) and WF(||) showed a definite difference, as shown in Fig. 10. Compacts WF(⊥), which had higher strength, fractured in the transparticle mode, while compacts WF(||) fractured in the interparticle mode.

3.4. Comparison with amorphous alloy ribbon

Tensile tests were carried out on amorphous alloy ribbons and the results were compared with the compressive strength of the amorphous alloy compacts (Fig. 7). The temperature dependence of tensile strength of the ribbons measured in this experiment is shown in Fig. 7. Results on tensile strength of an amorphous alloy ribbon and an amorphous alloy wire with similar composition published by other investigators, are also shown in the figure [17, 18].

Compressive strength of compacts EF and WF(⊥) was comparable to the tensile strength of the ribbon above 623 K. Compact WF(⊥), in particular, had a high compressive strength which corresponded to 80%–90% of tensile strength of the ribbons or the wire at room temperature. Transparticle fractures were observed in these cases, as mentioned earlier. In contrast, in those compacts of which compressive strength was considerably lower than the tensile strength of the ribbons or wire, interparticle fractures were mainly observed.

3.5. Elemental analysis of interparticle boundaries by EPMA

The features of the fracture surfaces described in Section 3.4, indicate that interparticle boundaries affected the bonding strength between powders and hence the mechanical properties of the compacts significantly. Elemental analysis of the interparticle boundaries in the as-consolidated compacts were performed by EPMA. The results are shown in Fig. 11. Peaks in oxygen intensity are considered to arise from oxide

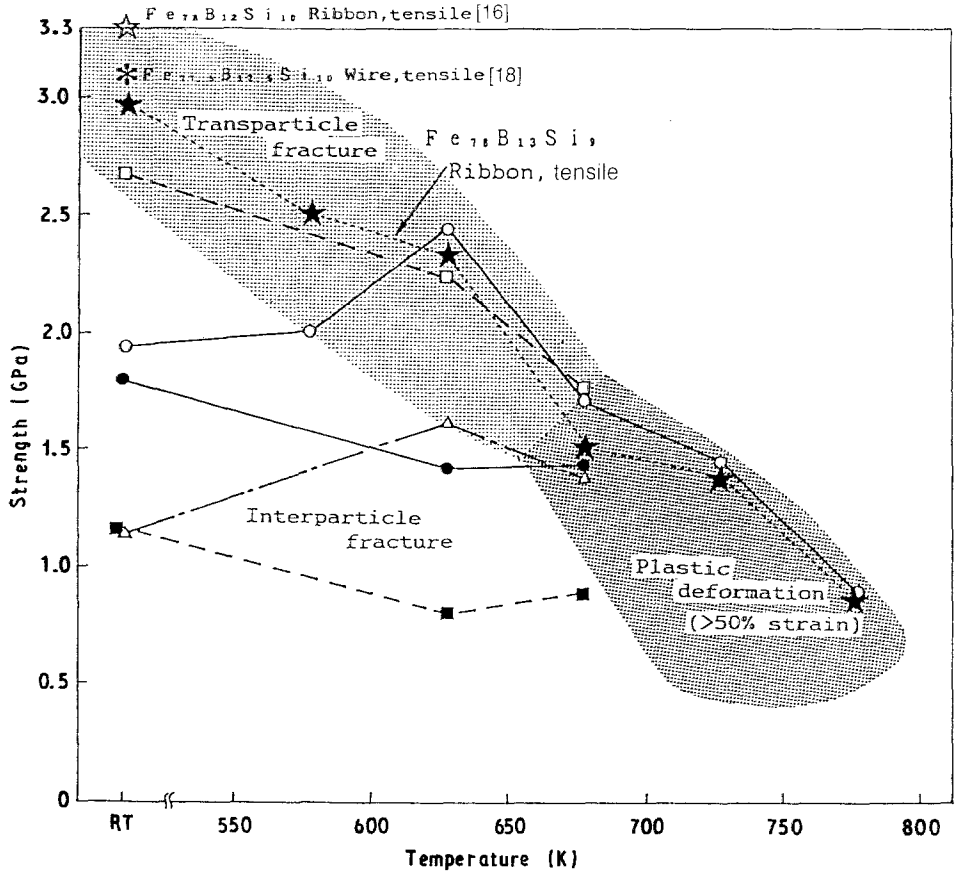

Figure 7 Temperature dependence of compressive strength of amorphous alloy compacts prepared by different consolidation techniques from different powders at $\dot{\varepsilon} = 8.33 \times 10^{-5}\,s^{-1}$. Yield stress or fracture stress is adopted as the compressive strength. Tensile strengths of amorphous alloy ribbons and an amorphous alloy wire with similar composition are also shown. (○) EF, (●) ES, (△) HF, (□) WF(⊥), (■) WF(∥).

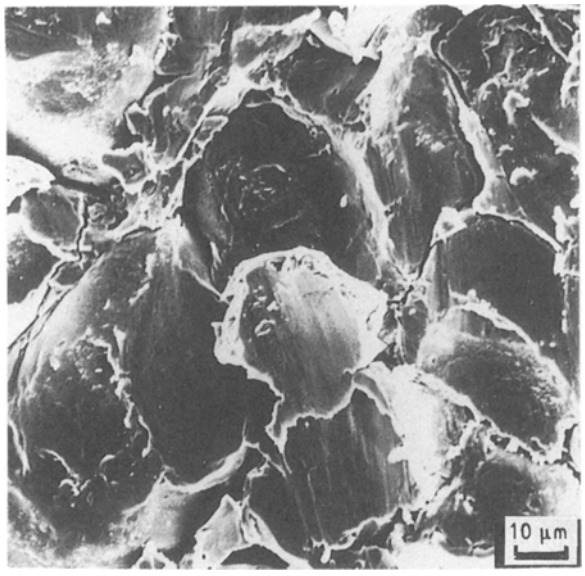

Figure 8 SEM images of the fracture surface of a spherical powder compact prepared by explosive consolidation (ES) when fractured at 623 K.

films in the interfaces between powders. In the explosively consolidated compacts (EF, ES), the oxygen peaks were comparatively low. In the compact EF, these peaks were especially low and broad. However, in the compacts prepared by high hydrostatic pressure consolidation (HF) and by warm extrusion (WF), higher oxygen peaks were observed.

4. Discussion

4.1. Deformation of amorphous alloy compacts

Explosively consolidated amorphous alloy compacts of $Fe_{78}B_{13}Si_9$ prepared from flaky powders (EF) could be deformed plastically, while preserving amorphous structure, to a strain of more than 50% at a strain rate of 8.3×10^{-5}–$2.5 \times 10^{-4}\,s^{-1}$ at 673 K. This large plasticity is coincident with an abrupt decrease in viscosity or softening of the amorphous alloy just below the crystallization temperature. The softening is also evident from the numerous elongated vein patterns, which are believed to be caused by shear stress, observed in the fracture surface after compression at 623 K (see Fig. 5c). Above 623 K yielding was observed, while fracture took place before yielding below 573 K.

Based on these results, it can be concluded that the compact EF softens above 623 K to such an extent that it can be deformed significantly prior to the fracture of the interparticle boundaries.

4.2. Effect of powder geometry

Study on the effect of powder geometry on the mechanical properties of explosively consolidated amorphous alloy compacts showed that flaky powder compacts (EF) had higher strength than spherical ones (ES). It has been generally recognized that bonding between metals during explosive consolidation takes place through the surface melting at the very moment

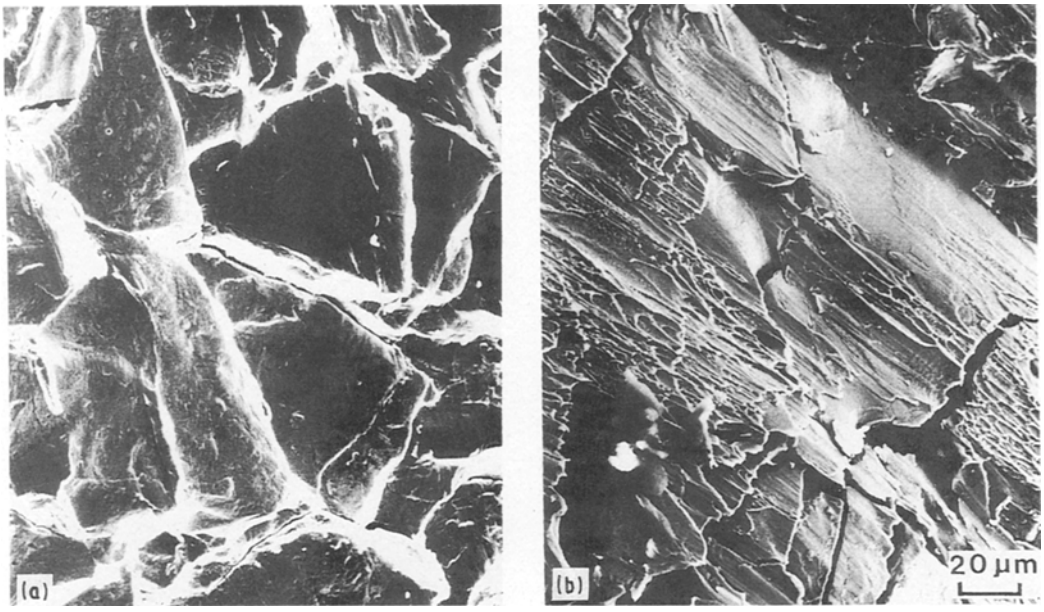

Figure 9 SEM images of fracture surfaces of amorphous alloy compacts prepared by high hydrostatic pressure consolidation (HF) compressed at (a) room temperature and (b) 623 K.

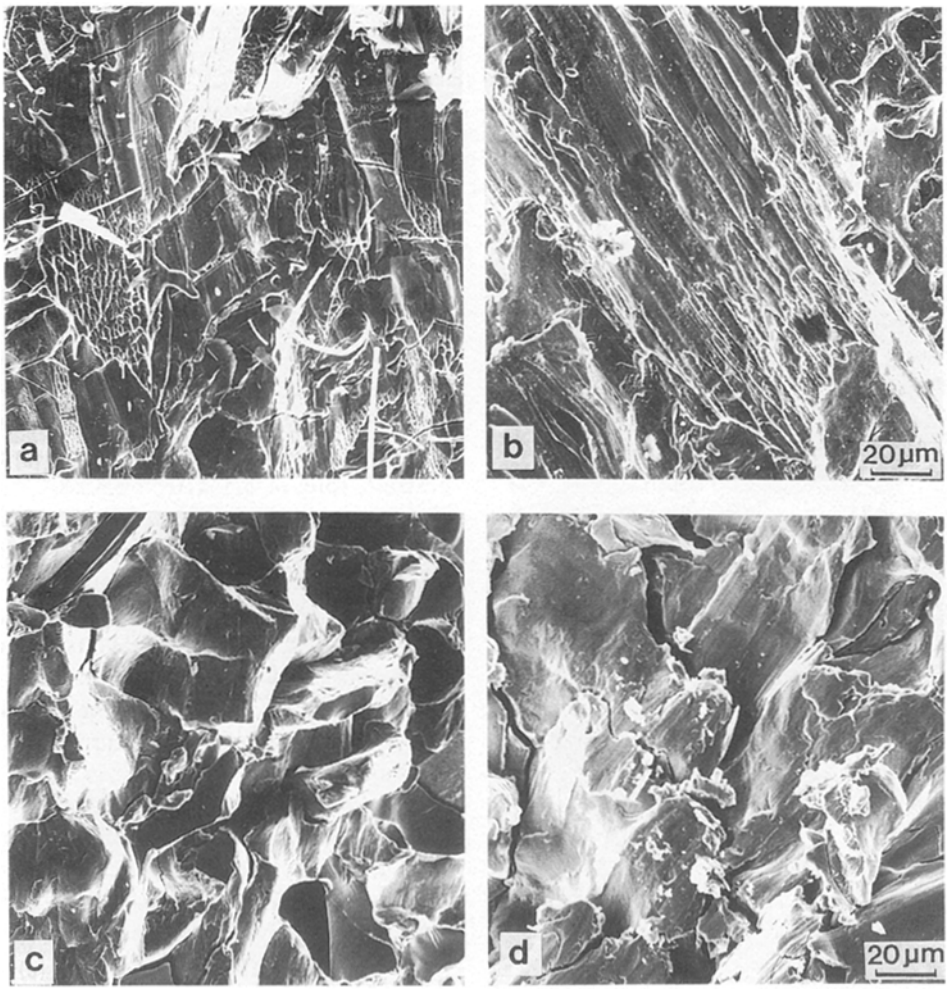

Figure 10 SEM images of fracture surfaces of amorphous alloy compacts prepared by warm extrusion when compressed at (a, c) room temperature and (b, d) 623 K (a, b) perpendicular to the extrusion axis, WF(⊥), and (c, d) parallel to the extrusion axis, WF(||).

that a shock wave propagates [19]. Broad peaks of oxygen observed in EPMA analysis on the flaky powder compacts (Fig. 11b) may indicate that the diffusion of oxygen had taken place during the melting of the surface of the powders. In contrast, EPMA analysis made on the spherical powder compact showed sharp and high peaks of oxygen (Fig. 11a). This seems to indicate that the surface melting during

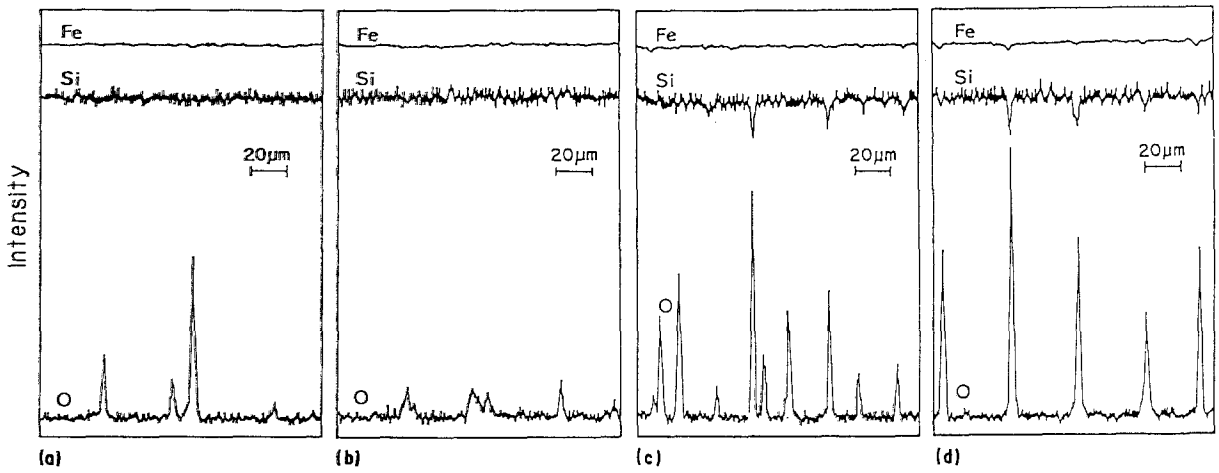

Figure 11 Results of EPMA analysis of amorphous alloy compacts prepared by (a) explosive consolidation from spherical powder (ES), (b) explosive consolidation from flaky powder (EF), (c) high hydrostatic pressure consolidation (HF), and (d) warm extrusion (WF).

the consolidation is incomplete in the case of the spherical powder.

This may be rationalized as follows. Because the spherical powders are packed very closely, they cannot move easily during explosive consolidation. This limited movement of powders generates only a limited heat which is insufficient to cause the surface melting of the powders. As a result, surface oxides of the starting powders persist in the interparticle boundaries, leading to interparticle fracture.

4.3. Effect of consolidation technique

Amorphous alloy compacts made by high hydrostatic pressure consolidation (HF) had lower strength than those prepared by explosive consolidation (EF). This difference is attributable to a difference in the bonding mechanism of powders between the two consolidation techniques. During the explosive consolidation, as has been already mentioned, it is believed that a surface melting of powders occurs and oxide films which coated the surfaces of the powders become dissociated, diffusing into the interior of the powders. During high hydrostatic pressure consolidation, however, such a surface melting is unlikely to occur. As a result, the surface oxide films remain on the surface, as is shown in Fig. 11c. It is natural to conclude that these oxide films lower the bonding strength between the powders, leading to a decrease in the compressive strength of the compacts.

Amorphous alloy compacts produced by warm extrusion (WF) showed a remarkable anisotropy in strength. This anisotropy can be explained by the anisotropy in morphology of powders in the compacts. When the flaky powders were warm extruded, they were aligned along the extruding direction through plastic flow. The compacts WF($\perp$) had the highest compressive strength and showed transparticle fracture when compressed perpendicular to the extrusion axis along which the powders were aligned. In contrast, the compacts WF($\parallel$) were fractured, at a considerably low strength, in the interparticle boundaries along the compression axis, namely parallel to the extrusion axis along which the powders were aligned. This fact indicates that the strength of interparticle boundaries has a major influence on the strength of the compacts, and the strength of the boundaries may be affected by the oxidation as shown in Fig. 11d.

In summary, in order to produce amorphous alloy compacts which have useful mechanical properties, not only the selection of consolidation technique and powder geometries but also the control of oxidation of interparticle boundaries in the compacts will be required.

5. Conclusions

Amorphous alloy compacts of $Fe_{78}B_{13}Si_9$ prepared by three different consolidation techniques from two kinds of amorphous alloy powder were deformed in compression at different temperatures and strain rates. The following results were obtained.

1. Mechanical properties of amorphous alloy compacts were significantly dependent on the consolidation technique and powder geometry.

2. Explosively consolidated compacts showed a compressive stress of 1.9–2.5 GPa below 623 K. The compacts prepared by high hydrostatic pressure consolidation showed lower compressive strength of 1.15–1.6 GPa than those prepared by explosive consolidation. The compacts produced by warm extrusion showed an anisotropy in the compressive strength; these had the highest compressive strength of 2.74 GPa at room temperature when compressed perpendicular to the extrusion axis, while they had a considerably lower compressive strength of 1.17 GPa when compressed parallel to the extrusion axis.

3. Explosively consolidated amorphous alloy compacts could be plastically deformed in compression to a strain of more than 50%, while preserving the amorphous state, at a temperature of 673 K and at a strain rate of 8.3×10^{-5}–$2.5 \times 10^{-4}\,s^{-1}$.

4. These differences in the mechanical properties are attributed to whether or not oxide films exist in the interparticle boundaries.

Acknowledgements

The authors thank Dr M. Araki and Mr Y. Kuroyama, Nippon Oil and Fats Co. Ltd, for the preparation of explosively consolidated amorphous alloy compacts, Professor M. Senoo, Mie University, and Dr A. Matsumuro, Nagoya University, for the advice on high hydrostatic pressure consolidation, and also Mr M. Akai, Nippondenso Co. Ltd, for the help in warm extrusion.

References

1. C. F. CLINE and R. HOPPER, *Scripta Metall.* **11** (1977) 1137.
2. D. G. MORRIS, *Met. Sci.* **14** (1980) 215.
3. H. H. LIEBERMANN, *Mater. Sci. Engng* **46** (1980) 241.
4. D. G. MORRIS, *J. Mater. Sci.* **17** (1982) 1789.
5. L. E. MURR, S. SHANKAR, A. W. HARE and K. P. STAUDHAMMER, *Scripta Metall.* **17** (1983) 1353.
6. P. KASIRAJ, D. KOSTKA, T. VREELAND Jr and T. J. AHRENS, *Non-Cryst. Solids* **61, 62** (1984) 967.
7. H. W. KUI, A. L. GREER and D. TURNBULL, *Appl. Phy. Lett.* **45**(6) (1984) 615.
8. D. RAYBOULD and C. F. CLINE, "Rapidly Solidified Crystalline Alloys" (1985) p. 111.
9. R. HASEGAWA and C. F. CLINE, in "Rapidly Quenched Metals", edited by S. Steeb and H. Warlimont (North-Holland, Amsterdam, 1985) p. 1667.
10. T. NEGISHI, T. OGURA, T. MASUMOTO, T. GOTO, K. FUKUOKA and Y. SYONO, *J. Mater. Sci.* **20** (1985) 399.
11. R. HASEGAWA, R. E. HATHAWAY and C. F. CHANG, *J. Appl. Phys.* **57-1** (1985) 3566.
12. D. G. MORRIS, in "Rapidly Quenched Metals", edited by S. Steeb and H. Warlimont (North-Holland, Amsterdam, 1985) p. 1751.
13. M. TAKAGI, Y. KAWAMURA, M. ARAKI, Y. KUROYAMA and T. IMURA, *Mater. Sci. Engng* **98** (1988) 457.
14. Y. KAWAMURA, M. TAKAGI, M. SENOO and T. IMURA, *ibid.* **98** (1988) 415.
15. Y. KAWAMURA, M. TAKAGI, M. AKAI and T. IMURA, *ibid.* **98** (1988) 449.
16. T. MASUMOTO, I. OHNAKA, A. INOUE and M. HAGIWARA, *Scripta Metall.* **15** (1981) 293.
17. T. MASUMOTO, *Sci. Rep. RITU* **A-26** (1977) 270.
18. M. HAGIWARA, A. INOUE and T. MASUMOTO, *Met. Trans.* **13A** (1982) 373.
19. D. RAYBOULD, *J. Mater. Sci.* **16** (1981) 589.

Received 15 October 1990
and accepted 25 March 1991